*Macromolecules* **2001,** *34,* 723−726

# Conformational Dynamics in a Methacrylate-Derived Radical: A Computational and EPR Study

**Martin Spichty,[†] Bernd Giese,[†] Akikazu Matsumoto,[‡] Hanns Fischer,[§] and Georg Gescheidt*[,†]**

*Department of Chemistry, University of Basel, Klingelbergstrasse 80, CH-4056 Basel, Switzerland; Department of Applied Chemistry, Osaka City University, Sugimoto, Sumiyoshi-ku, Osaka 558, Japan; and Physikalisch Chemisches Institut, University of Zürich, Winterthurerstrasse 190, CH-8092 Zürich, Switzerland*

*Received July 13, 2000; Revised Manuscript Received November 14, 2000*

ABSTRACT: Dynamic phenomena are established for the [$D_3$]methyl (2*SR*,3*RS*)-2-methyl-4,4,4-trichlorobutanoate-2-yl radical (**1**). This is revealed by EPR spectroscopy and quantum chemical calculations. The minimum conformations **B** and **D** of **1** possess planar radical centers and are sepearated by an energy barrier of 12.0 ± 1.8 kJ·mol$^{-1}$ (experimental; calculated, 11.0 kJ·mol$^{-1}$).

## Introduction

Radical polymerization is an amply utilized method in industry. Therefore, it is not surprising that radicals occurring in the course of these reactions have been intensively studied. Many of these studies were performed with the help of EPR methods, and one can even regard the publications on such radicals as historical examples for the observation of basic phenomena like the characteristic sizes of $\beta$-proton hyperfine coupling constants or line broadening due to conformational dynamics.[1−5]

The initiation and the growth of the radical chain cover a wide range of reaction rates. [6−9] What are the factors governing the properties of the propagating polymer? Clearly the (stereo)selectivity for the monomer addition is controlled by steric factors, and therefore, the geometry or, more accurately, the preferred conformation of a radical is decisive.[10−12] The conformation of the growing radical chain directs the orientation of the adding monomers, i.e., the sterical demand of the α-substituents and $\beta$-substituents directs the selectivity of additions. This is also connected to the penultimate-unit effect in polymerization reactions.[13−18]

Radicals of type **I** and **II** represent models for the addition of methacrylares and acrylates to a radical R$^\bullet$ (Chart 1). Their conformations were studied by EPR spectroscopy and several examples can be found in the literature.[1−5,19,20] A more recent analysis of EPR spectra obtained from acrylate-derived radicals, e.g., [$D_3$]methyl (2*SR*,3*RS*)-2-methyl-4,4,4-trichlorobutanoate-2-yl radical (**1**) presents some unexpected conclusions: Two distinctly different radicals, a high- and a low-temperature species with a pyramidalized geometry at the radical center are anticipated.[21] Such structures would imply a reactivity which should be definitely different from that of a planar radical center deduced from the earlier studies, both in terms of sterical interactions and in terms of a higher reactivity caused by an increased $\sigma$-character of the radical center.

**Chart 1**

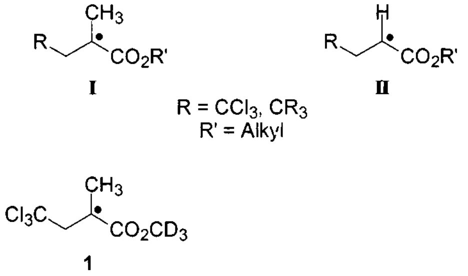

Are such bent radical geometries really likely? Within the last couple of years it was shown that, in particular, calculations on the density functional level of theory[22] lead to reliable predictions of radical structures and EPR parameters.[23−26] Combining the predictions from theory with temperature-dependent EPR spectra, we wish to reexamine the structure of **1** and related radicals.

## Results and Discussion

In Figure 1, the EPR spectra obtained during photolysis of **2** are shown together with the corresponding simulations. Above 273 K no dramatic changes in the EPR signal patterns are notable and a perfect match between the experimental and the simulated EPR spectrum is attained (Figure 1) with a $^1$H isotropic hyperfine coupling constant, hfc, of 1.12 mT attributable to two equivalent protons in the $\beta$-position ($H_{\beta'}$, $H_{\beta''}$) in respect to the radical center. The second $^1$H hfc of 2.357 mT of three equivalent protons consequently stems from the protons of the α-methyl group.

Below 243 K, the central lines of the 1:2:1 pattern (marked with an asterisk in Figure 1) attributed to the two (yet equivalent) $\beta$-protons begin to broaden showing unusual intensity ratios while the outermost lines (marked with a square) remain constant. Previously, this observation was interpreted in terms of two different radicals being present where one of the radicals reversibly disappears at low temperatures.[21] Simulations of the experimental spectra, however, have not been shown. Reexamination of the former results rather points to dynamical phenomena being responsible for the (line width) alternations in the EPR signals:[27] This

---

* Corresponding author. Telephone: +41 61 267 38 32. Fax: +41 61 267 38 55. E-mail: georg.gescheidt@unibas.ch.

[†] University of Basel.

[‡] Osaka City University.

[§] University of Zürich.

10.1021/ma001217g CCC: $20.00

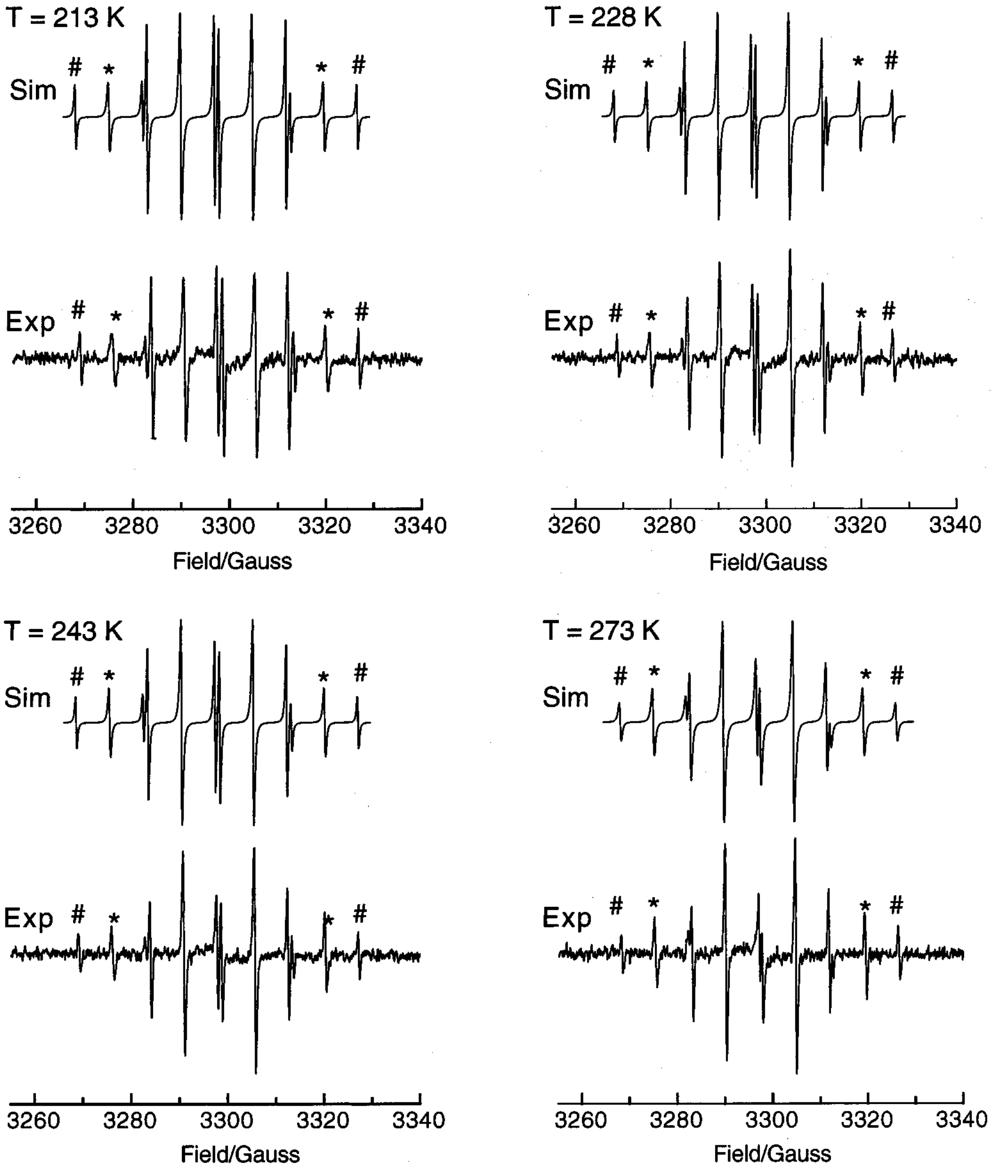

**Figure 1.** EPR spectra of **1** at 213, 228, 243, and 273 K and their simulations.

behavior is distinctive for a dynamical two-site exchange process often observed in EPR spectra of alkyl radicals. Obviously such EPR spectra can be simulated (Figure 1) with the assumption of a two-jump model.

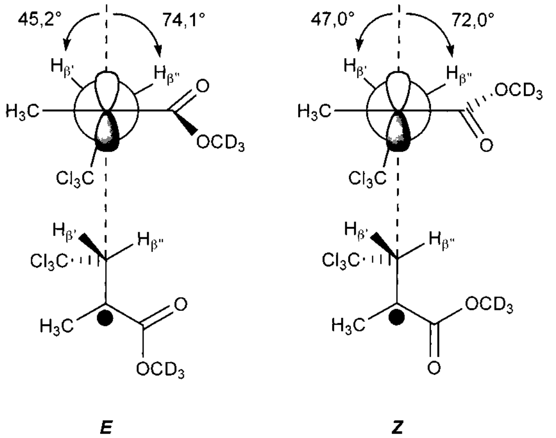

**Figure 2.** "*E*" and "*Z*" isomers of radical **1** including dihedral angles of the UB3LYP/6-31G* optimized structures.

Whereas the fast-exchange limit—where the rotation of the $CCl_3CH_2$ moiety in respect to the radical center is fast on the hyperfine time scale—is reached at 273 K ($^1H_\beta$ hfc of 1.12 mT for two equivalent protons), the slow exchange regime with two *non*equivalent $H_\beta$ cannot be reached. But which hfcs should be used for the conformation of minimum? It has been shown that particularly density functional theory calculations with the hybrid functional B3LYP are able to give rather precise predictions for the minimum geometry of organic radicals together with the corresponding hfcs.[26] Computations of **1** on the UB3LYP/6-31G* level reveal two isomers. In one isomer, denoted "*Z*", the carbonyl group of the ester moiety is oriented toward the α-methyl group, but is reversed in the "*E*" isomer (Figure 2). In both cases the radical center is planar. The $\beta'$ protons are twisted out of the nodal plane of the radical center by 45 and 47°, respectively; consequently, the angles between the $p_z$ axis of the radical center and the remaining $\beta''$-H atom are 74 and 72° (Figure 2). The calculations indicate that the *E* isomer is more stable than the *Z* by only 1.4 kJ·mol$^{-1}$.

The calculated $^1H$ hfcs for the minimum conformations of the *E* and *Z* isomers are given in Table 1 together with the values which take into account

**Table 1. Experimental and Calculated hfcs (in mT) for Radical 1**

| | | "*E*" isomer | | "*Z*" isomer | |
|---|---|---|---|---|---|
| position | exptl[a] $T = 273$ K | min $T = 0$ K | Boltzmann $T = 273$ K | min $T = 0$ K | Boltzmann $T = 273$ K |
| $\beta'$ } $\beta$ | 1.117 | 1.65 | 1.16 | 1.53 | 1.15 |
| $\beta''$ | | 0.39 | | 0.46 | |
| α-Me | 2.357 | 2.23 | 2.22 | 2.21 | 2.20 |

[a] The *g* factor is 2.0043 for all temperatures.

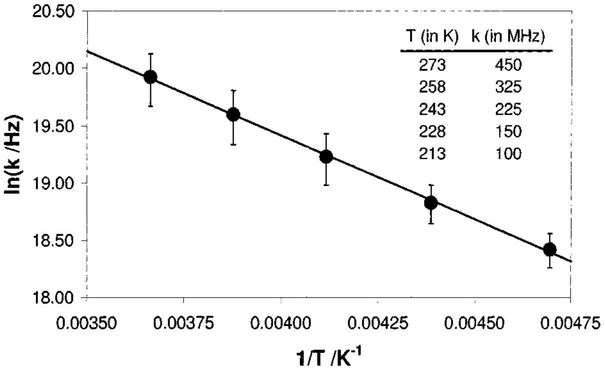

**Figure 3.** Arrhenius plot for radical **1**. $k$ = exchange rate, $T$ = temperature.

additionally populated rotamers of the $CD_3COOCH_3C^{\bullet}{-}CH_2CCl_3$ bond (see below) given by the Boltzmann distribution. It is apparent that the $^1H$ hfcs are virtually identical for both isomers. Therefore, a differentiation between them is not possible by means of the experimental data. The calculated, Boltzmann averaged $\beta$ hfc at $T = 273$ K is almost identical for both isomers and the value of 1.15–1.16 mT is in excellent agreement with the experimental counterpart of 1.12 mT obtained in the high-temperature EPR spectra. The same is apparent for the $^1H$ hfc of the α-methyl group (calculated, 2.20–2.21; experimental, 2.357 mT; Table 1).

With the calculated hfcs values of 0.4 and 1.7 mT (minimum conformation of the *E* isomer) for the two different $H_\beta$ in the slow-exchange limit (i.e.) low temperature, the experimental EPR spectra could be simulated for the entire range of temperatures in a straightforward way. Using the exchange frequencies established by the spectral simulations, the Arrhenius plot (Figure 3) yields an activation energy of $12.0 \pm 1.8$ kJ·mol$^{-1}$ and a frequency factor of $\log(A/s^{-1}) = 10.94 \pm 0.41$. Figure 4 shows the energy profile for the rotation along the $CD_3COOCH_3C^{\bullet}{-}CH_2CCl_3$ bond in the *E* isomer calculated on the UB3LYP/6-31G* level. The relative electronic energy is plotted vs the dihedral angle $\gamma$-(1,2,3,4) from 0 to 360°. The profile for the *Z* isomer is not presented because it is only marginally differing from that for the *E*. The two minimum conformations **B** and **D** represent "eclipsed" structures, separated by an energy barrier of 11.0 kJ·mol$^{-1}$ (9.7 kJ·mol$^{-1}$ in the "*Z*" isomer) via "gauche" conformation **C**. This value closely resembles the experimental $E_a$ of $12.0 \pm 1.8$ kJ·mol$^{-1}$. The sterically congested conformer **A** is not populated.

In conclusion, our study shows that the radical **1** indicates dynamical phenomena between conformers **B** and **D**. These conformers direct the addition of the next alkene monomer being responsible for the stereoselectivity of the polymerization. A similar dynamic behavior has been established for a number of related radicals.[28] Analogous phenomena are also clearly visible in the EPR spectra of several other derivatives of type **II** reported in the previous study.[21]

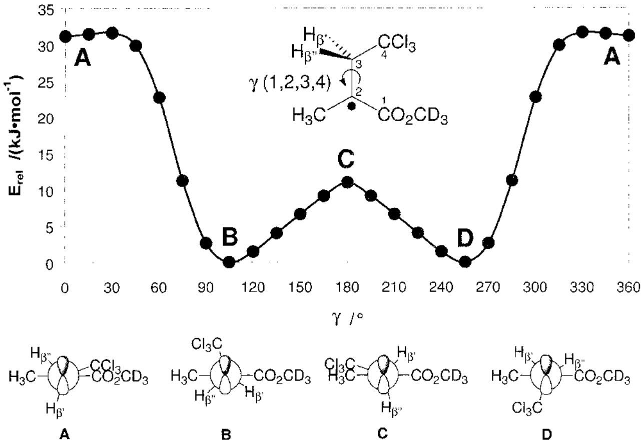

**Figure 4.** Energy profile for the rotation around the $CD_3$-$COOCH_3C^{\bullet}{-}CH_2CCl_3$ bond in the "*E*" isomer of radical **1**.

**Scheme 1**

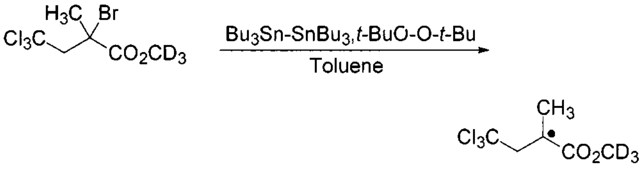

## Experimental Section

The EPR spectra were recorded on a Bruker ESP 300E spectrometer equipped with a variable temperature unit. Radical **1** was generated by photolysis of **2** (irradiation with a Hg/Xe high-pressure lamp (Hanovia SP 1000, IR Filter) within the cavity of the EPR spectrometer; Scheme 1). Simulations of the EPR spectra were done with a program by J. Heinzer (ETH Zurich). Quantum chemical calculations were performed with Gaussian 94.[29]

**Acknowledgment.** We thank the Swiss National Science Foundation and Ciba Speciality Chemicals (G.G.) for financial support.

**Supporting Information Available:** Table of coordinates of the optimized geometries of "*Z*"- and "*E*"-**1**. This material is available free of charge via the Internet at http://pubs.acs.org.

## References and Notes

(1) Schneider, E. E. *Nature* **1951**, *168*, 645.
(2) Fischer, H. *Polym. Lett.* **1964**, *2*, 529.
(3) Fischer, H. *Z. Naturforsch.* **1964**, *19a*, 866.
(4) Fischer, H. *Kolloid-Z. Z. Polym.* **1965**, *206*, 131.
(5) Fischer, H. *Proc. R. Soc. London, Ser. A* **1967**, *302*, 321.
(6) Gatlik, I.; Rzadek, P.; Gescheidt, G.; Rist, G.; Hellrung, B.; Wirz, J.; Dietliker, K.; Hug, G.; Kunz, M.; Wolf, J.-P. *J. Am. Chem. Soc.* **1999**, *121*, 8332.
(7) Heberger, K.; Walbiner, M.; Fischer, H. *Angew. Chem.* **1992**, *104*, 651.
(8) Weber, M.; Fischer, H. *Helv. Chim. Acta* **1998**, *81*, 770.
(9) Zytowski, T.; Fischer, H. *J. Am. Chem. Soc.* **1997**, *119*, 12869.
(10) Curran, D. P.; Porter, N. A.; Giese, B. *Stereochemistry of Radical Reactions: Concepts, Guidelines, and Synthetic Applications*; VCH: Weinheim, Germany, 1996.
(11) Thoma, G.; Curran, D. P.; Geib, S. V.; Giese, B.; Damm, W.; Wetterich, F. *J. Am. Chem. Soc.* **1993**, *115*, 8585.
(12) Roth, M.; Damm, W.; Giese, B. *Tetrahedron Lett.* **1996**, *37*, 351.
(13) Wu, L. M.; Fischer, H. *Helv. Chim. Acta* **1983**, *66*, 138.
(14) Deb, P. C.; Meyerhoff, G. *Eur. Polym. J.* **1984**, *20*, 713.
(15) Fukuda, T.; Kubo, K.; Ma, Y. D. *Prog. Polym. Sci.* **1992**, *17*, 875.

(16) Yamada, B.; Westmoreland, D. G.; Kobatake, S.; Konosu, O. *Prog. Polym. Sci.* **1999**, *24*, 565.

(17) Spichty, M.; Weber, M.; Fischer, H.; Giese, B. Manuscript in preparation.

(18) Coote, M. L.; Davis, T. P.; Radom, L. *Macromolecules* **1999**, *32*, 2935.

(19) Ingram, D. J. E.; R.; S. M. C.; G.; T. M. *Trans. Faraday Soc.* **1958**, *54*, 409.

(20) Symons, M. C. R. *J. Chem. Soc.* **1963**, 1186.

(21) Matsumoto, A.; Giese, B. *Macromolecules* **1996**, *29*, 3758.

(22) Parr, R. G.; Yang, W. *Density-functional theory of atoms and molecules*; Oxford University Press: New York, 1989.

(23) Gauld, J. W.; Eriksson, L. A.; Radom, L. *J. Phys. Chem. A* **1997**, *101*, 1352.

(24) Gano, J. E.; Jacob, E. J.; Sekher, P.; Subramaniam, G.; Eriksson, L. A.; Lenoir, D. *J. Org. Chem.* **1996**, *61*, 6739.

(25) Engels, B.; Eriksson, L. A.; Lunell, S. *Adv. Quant. Chem* **1996**,.

(26) Batra, R.; Giese, B.; Spichty, M.; Gescheidt, G.; Houk, K. N. *J. Phys. Chem.* **1996**, *100*, 18371.

(27) Weil, J. A.; Wertz, J. E.; Bolton, J. R. *Electron Paramagnetic Resonance*; Wiley: New York, 1994.

(28) Matsumoto, A. *J. Polym. Sci.* **1999**, *37*.

(29) Frisch, M. J.; Trucks, G. W.; Schlegel, H. B.; Gill, P. M. W.; Johnson, B. G.; Robb, M. A.; Cheeseman, J. R.; Keith, T.; Petersson, G. A.; Montgomery, J. A.; Raghavachari, K.; Al-Laham, M. A.; Zakrzewski, V. G.; Ortiz, J. V.; Foresman, J. B.; Peng, C. Y.; Ayala, P. Y.; Chen, W.; Wong, M. W.; Andres, J. L.; Replogle, E. S.; Gomperts, R.; Martin, R. L.; D. J. Fox; Binkley, J. S.; Defrees, D. J.; Baker, J.; Stewart, J. P.; Head-Gordon, M.; Gonzalez, C.; Pople, J. A. *Gaussian 94, Revision B.3*; Gaussian, Inc.: Pittsburgh, PA, 1995.

MA001217G